Origin of the linear tunneling conductance background

J. R. Kirtley
IBM Thomas J. Watson Research Center, P.O. Box 218, Yorktown Heights, New York 10598

S. Washburn
Department of Physics, University of North Carolina, Chapel Hill, North Carolina 27599

D. J. Scalapino
Department of Physics, University of California, Santa Barbara, California 93106
(Received 12 July 1991)

Tunnel junctions often have conductances that are linear in voltage over wide voltage ranges. Although this linear conductance background has received much attention recently in connection with the high-T_c superconductors, it is found in many systems. Previous work has shown that the discontinuity in slope of the linear conductance background at zero bias is thermally smeared by $\sim 5kT$, consistent with inelastic tunneling from a broad, flat continuum of states. In this paper we concentrate on a particular system, junctions with Cr_2O_3 in the barrier region, in which the size of the effect can be adjusted by changing the barrier composition. Careful analysis of the Pb strong-coupling phonon structure in Al-Cr_2O_3-Pb junctions is consistent with the inelastic-tunneling hypothesis, and inconsistent with a voltage-dependent matrix-element explanation for this effect. Suppression of the Al gap signature, as well as Zeeman splitting of the conductance background near zero bias, indicates that strong spin interactions occur in the barrier region in these junctions. We present Monte Carlo simulations of multiple-scattering strong inelastic tunneling to explain the very wide voltage range over which the linear background occurs. We argue that the same basic mechanism is probably responsible for the linear background in junctions involving high-T_c junctions as for the junctions studied in detail here.

Tunneling measurements of the high-T_c superconductors often show conductance backgrounds that increase linearly in voltage over hundreds of millivolts.[1,2] Although this linear background in tunneling into the high-T_c superconductors has been interpreted in several different ways, much emphasis has been placed on models in which this background reflects the density of states of the bulk of the high-T_c material. Anderson and Zou[3] interpreted the tunneling data in terms of the resonating-valence-band (RVB) model. In this picture, the tunneling carriers excite both charge and spin degrees of freedom in the high-T_c superconductor. Integration over one of these degrees of freedom leads to conduction linear in voltage. Varma *et al.*[4] interpreted the linear conductance background using a model in which strong inelastic scattering modified the effective tunneling density of states. Phillips[5] attributed the linear conduction background to tunneling into localized states. In an earlier paper,[6] two of the present authors observed that the linear conduction background actually occurs in many different kinds of junctions, and showed that, for several of these, including junctions involving high-T_c superconductors, the discontinuity in slope at zero bias is thermally smeared by $\sim 5kT$, consistent with inelastic tunneling from a broad continuum of states.[7,8] They proposed a particular microscopic mechanism for this inelastic scattering suitable for the cuprate high-T_c superconductors; strong inelastic scattering from spin fluctuations. In this paper, we present additional experimental data on the linear conduction background, concentrating on planar junctions with Cr_2O_3 in the barrier region. Unlike junctions involving high-T_c materials, these junctions offer well-defined, reproducible, variable composition tunneling barriers. Suppression of the Al gap signature by small quantities of Cr_2O_3 in the barrier region of Al-Al_2O_3-Pb junctions indicates that there is strong spin-dependent scattering in these samples. The inclusion of Cr_2O_3 in the barrier region of Al-Al_2O_3-Pb junctions can increase the size of the linear conduction background by orders of magnitude, indicating that the presence of a linear conductance background does not necessarily imply unusual properties of the bulk of the electrodes making up the junction. A careful analysis of the strong-coupling Pb phonon structure in Al-Al_2O_3-Cr_2O_3-Pb junctions is consistent with the inelastic hypothesis, and inconsistent with the conventional analysis, which is only appropriate if the conduction background is due to voltage-dependent matrix-element effects. The magnetic field dependence of the linear conduction background in Cr-Cr_2O_3-Pb junctions exhibits Zeeman splitting with an energy scale consistent with accepted g factors for Cr_2O_3. We compare our measurements with the predictions of the inelastic-tunneling model, using antiferromagnetic magnons as the energy-loss mechanism, and find reasonable agreement. Finally, the wide voltage range over which the linear conduction background extends—wider than might be expected from such energy-loss mechanisms as acoustic phonons or antiferromagnetic magnons—may be an indication of emission of multiple elementary excitations in the tunneling process. We

present here Monte Carlo calculations of conductance-voltage characteristics in the presence of strong inelastic tunneling with multiple-magnon emission. These calculations show nearly linear conduction backgrounds for sufficiently strong inelastic scattering. These calculations also exhibit asymmetry of the conductance background with respect to voltage with properties similar to experimental observations. Although we concentrate in this paper on junctions with Cr_2O_3 in the barrier region, the size of the effect reported here spans the range observed for tunneling into the high-T_c cuprate superconductors, the thermal smearing is identical within experimental error for the two systems, and there is good reason to believe that there are antiferromagnetic interactions in the barrier region in both cases. We argue that these results are therefore relevant to tunneling measurements of the high-T_c superconductors.

Linear conductance backgrounds over wide voltage ranges have previously been observed in a wide variety of tunneling systems, including Cr-Cr_2O_3-Ag junctions,[9,10] Al-Al_2O_3-Pb junctions, both undoped[6] and doped with Cr,[11] Cu,[12] Ti,[12] and organic materials[13] in the barrier region, junctions with iron oxide in the barrier region,[14] Al-Al_2O_3-$Ge_{1-x}Au_x$ junctions,[15] and GaAs-$Al_xGa_{1-x}As$-GaAs heterojunction tunnel junctions.[16] Figure 1 demonstrates several remarkable aspects of this effect. First, the tunneling conductance can be linear over hundreds of meV's. Second, the slope of the linear conduction background can be large. Third, there is a discontinuity in the slope of the conductance at zero bias that can be sharp at low temperatures. Fourth, the slope of the linear conductance background is often significantly different for opposite voltage biases. Finally, the linear conductance background appears in junctions with very different electrode compositions. As shown in Fig. 1, although the size of the effect changes by several orders of magnitude from system to system, when scaled the data appear very similar.

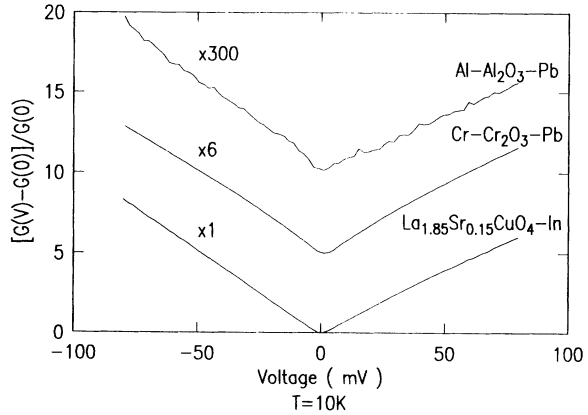

FIG. 1. Normalized dynamic conductance-voltage curves for a thin-film Al-Al_2O_3-Pb junction, a thin-film Cr-Cr_2O_3-Pb junction, and a $La_{2-x}Sr_xCuO_4$-In pressed contact junction. Although the size of the linear conduction background varies by nearly 3 orders of magnitude, when scaled the data appear quite similar. The voltages displayed are the Pb voltages for the thin-film junctions, and the $La_{2-x}Sr_xCuO_4$ voltage for the pressed contact junction.

A number of explanations for the linear conductance background in tunneling into the high-T_c superconductors have been proposed. The simplest such explanation involves the voltage dependence of the elastic-tunneling matrix elements.[14,17] Good fits of point-contact tunneling data into the high-T_c superconductors can be made using conventional tunneling theory with a trapezoidal model for the tunneling barrier potential. However, there are three difficulties with this simple explanation. First, extremely low effective tunneling barrier heights (less than 100 mV) are required to fit the data. Second, it is very difficult to reproduce the sharpness of the experimentally observed discontinuities in the slope of the conductance at zero voltage (see Fig. 1) using this model. Third, the experimentally observed thermal smearing of the "kink" in conductance at zero bias is larger than predicted by a simple elastic-tunneling model.[6]

A second possible mechanism for the linear conductance background is charging effects in the tunneling barrier.[18–20] Zeller and Giaever[21] showed that such effects give linear conduction backgrounds for a distribution of effective capacitances in the tunneling region. There are two drawbacks to this explanation. First, extremely small capacitances are required to explain the large voltage range over which the linear conductance occurs. Second, the effect occurs for systems in which it appears unlikely that isolated metallic regions are included in the barrier region. It should be pointed out, however, that the thermal smearing of the linear conductance background[6] is consistent with a charging model.[20]

A third possible model for the linear conductance background is a modification of the effective tunneling density of states.[22] This explanation does not appear to be sufficiently general to apply to the broad variety of systems in which the linear conductance background occurs. For example, it is difficult to understand how correlation effects in the electrodes can be important in the Al-Al_2O_3-Cr_2O_3-Pb junctions described below. (For convenience, we will refer to the oxide of aluminum as Al_2O_3 and that of Cr as Cr_2O_3. It is commonly believed that these are the predominant stoichiometries of the oxides formed on these metals under the conditions we used: the precise chemical composition of the tunneling barriers is unimportant to the thrust of this paper.) In addition, in junctions with Cr_2O_3 in the barrier region the size of the linear conduction background is controlled by variations in the composition of the tunneling barrier, as opposed to variations in the electrode composition. These experiments make it clear that the presence of a linear tunneling conduction background does not necessarily indicate unusual properties intrinsic to the electrodes.

The fourth possible mechanism for the linear conductance background, which we wish to explore in this paper, in inelastic tunneling from a broad, flat distribution of inelastic modes in the barrier region.[6] For discrete modes in the tunneling barrier there is a sharp increase in the tunneling conductance each time the energy eV gained by an electron in traversing the tunneling region exceeds a characteristic loss energy $\hbar\omega$.[23] If there are broadband energy-loss modes in the barrier region, in-

elastic tunneling will result in a continuous increase in conductance: at zero temperature, for normal metal electrodes, and if we ignore the dependence of the inelastic tunneling matrix elements on initial and final electron momenta, the inelastic contribution to the conductance is given by

$$dI_i(V)/dV \sim \int_0^{eV} d(\hbar\omega) F(\omega) , \quad (1)$$

where $F(\omega)$ is the spectral distribution of inelastic-scattering modes in the barrier region. Inelastic-tunneling processes with energy loss to broadband excitations have been suggested as a cause of voltage-dependent conductance backgrounds.[24] In our model, the linear conduction background is indicative of a flat distribution of inelastic-scattering states. Given the striking diversity of tunneling systems in which the linear conduction background is observed, it is unlikely that a single microscopic inelastic-scattering mechanism is responsible. This is in analogy with $1/f$ noise in metals. Dutta, Dimon, and Horn showed that noise with a spectral distribution roughly inversely proportional to frequency results from a flat distribution of trap activation energies.[25] Different systems can have different trap mechanisms: the common factor is the flat distribution of trap energies.

The existence of a continuum of inelastic loss modes in typical tunneling barriers, in addition to the discrete modes first identified by Jaklevic and Lambe,[23] is made plausible by Fig. 2, which shows the second derivative of the current-voltage characteristic d^2I/dV^2 from the same planar Al-Al_2O_3-Pb junction as in Fig. 1. The curves in this figure are not shifted vertically for clarity: the zero in d^2I/dV^2 is well below any smooth curve that can be drawn through the data, and there is significant asymmetry in the curves with respect to reversal of the voltage polarity. In Fig. 2 there is no applied magnetic field, so that the very large structures at low voltages due to the Pb superconducting gap and Pb electron-phonon strong-coupling modifications of the Pb density of states are apparent. The structures at ~ 100 meV are due to inelastic scattering from Al_2O_3 phonons and hydroxyl ions in the barrier region. The features at ~ 350 meV are from CH stretching modes, and the features at ~ 450 meV are from OH stretching modes, from residual hydrocarbons, and hydroxyl ions in the barrier.[26] Although there are clear indications of impurities in the barrier region of this junction from the discrete inelastic electron tunneling features, the size of these features indicates that there is less than a monolayer of such impurities.[27] As can be seen in Fig. 1, the conductance of this junction increases nearly linearly in voltage below ~ 200 mV, with a discontinuity in slope at $V=0$. Part of this increase can be attributed to conductance steps from discrete vibrational modes in the barrier region. An estimate of their relative contribution can be made by integrating the area between the data in Fig. 2 and a smooth background curve, indicated by the dashed lines in Fig. 2. Part of the conductance increase at high biases is due to the lowering of the effective tunneling barrier by the applied bias. However, the total change in conductance with voltage at low biases (<200 meV) is an order of magnitude larger than can be attributed to the indentifiable discrete inelastic energy-loss features, or barrier effects. We suggest that this additional contribution to the background conductance is due to inelastic scattering from a broad continuum of states.

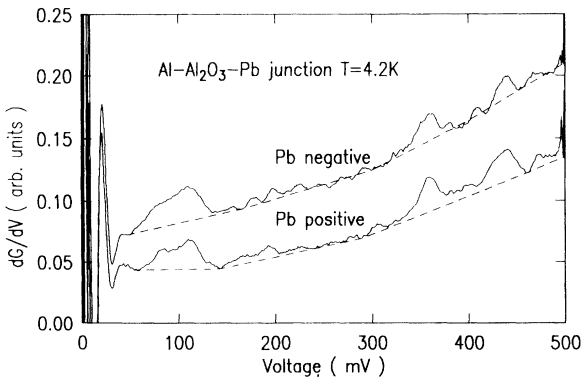

FIG. 2. Dynamic derivative of the conductance for the Al-Al_2O_3-Pb junction of Fig. 1 for the two opposite voltage polarities. There are small peaks associated with distinct vibrational modes in the barrier, but also an asymmetric offset to these curves which we associate with a broad continuum of states.

One distinction that can be drawn between the inelastic-tunneling model and the density-of-states models is that the size of the background might be expected to be dependent only on changes in the composition of the electrode material for the density-of-states model, whereas the size of the background might be expected to be most strongly dependent on changes in the composition of the tunneling barrier in the inelastic model. Tunneling junctions of the form Al-Al_2O_3-Cr_2O_3-Pb make a particularly attractive system for testing this distinction. Large linear conduction backgrounds in Cr-Cr_2O_3-Pb junctions were first noted by Shen and Rowell.[9] Rochlin and Hansma[10] attempted to determine whether this background was due to the Cr metal electrode or due to oxidized chromium in the barrier region by forming Al-Cr_2O_3-Sn junctions. They found that junctions formed by oxidizing a 60-Å overlay of chromium on Al films showed the same backgrounds as samples formed simply by oxidizing Cr thin films. Rochlin and Hansma[10] argued that there was no unoxidized chrome in the barrier region of their hybrid junctions. In order to ensure that this is indeed true in our samples, we have repeated these measurements for a series of thicknesses of Cr overlays. Our samples were fabricated by evaporating a series of 200-Å-thick, 1-mm-wide Al thin films through a mechanical mask onto glass slides in a cryopumped vacuum evaporator at 10^{-7} torr. Without breaking vacuum, varying thicknesses of Cr were evaporated onto successive Al stripes by moving a shutter. The films were then oxidized in air at 200 °C for 20 min and then returned to the evaporator for a cross stripe of Pb 1-mm-wide and 2000-Å thick.

Figure 3 shows conductance-voltage characteristics from such Al-Al_2O_3-Cr_2O_3-Pb junctions for a series of different barrier compositions. The labels correspond to thicknesses of Cr deposited on the Al film before oxidation, as measured with a quartz crystal microbalance. It

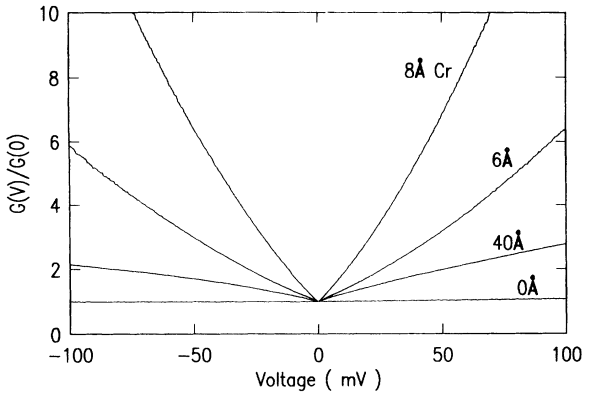

FIG. 3. Normalized dynamic conductance curves for a set of Al-Al_2O_3-Cr_2O_3-Pb junctions with different mass thicknesses of Cr evaporated on the Al thin films before oxidation. The size of the linear conduction background changes by nearly 3 orders of magnitude upon inclusion of Cr_2O_3 in the barrier region.

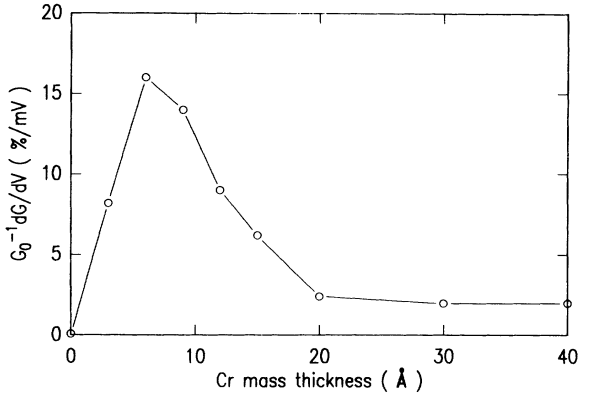

FIG. 4. Dependence of the slope of the linear conduction background for a particular set of Al-Al_2O_3-Cr_2O_3-Pb junctions, as a function of the mass thickness of Cr evaporated on the Al before oxidation. For all of the sets we studied, the slope peaked sharply at a Cr mass thickness of about 10 Å.

is unlikely that the coverage of Cr on the Al films is complete for our thinnest Cr samples. However, the resistance of these samples with Cr deposited on them are an order of magnitude smaller than without Cr. This indicates that the Cr tends to limit tunneling barrier growth in the Al so that current tends to flow more strongly in the areas with Cr on them. It is unlikely that regions of unoxidized Cr metal exist for the thinnest Cr samples, since Cr films are estimated to form oxide films 50-Å thick under the conditions we used.[10] We tested for possible effects due to unoxidized Cr in our samples by reordering the sample fabrication procedure: the Al films were oxidized in air at 200 °C for 20 min, varying thicknesses of Cr were evaporated, and the composite films were exposed to room temperature air for an hour before being returned to the vacuum evaporator for completion with a Pb electrode. For these partially oxidized Cr samples, steps in conductance periodic in voltage, indicative of charging effects from small metallic particles in the barrier region,[28] were clearly discernible, and the conductance background increased with voltage much faster than linearly. The absence of these effects in our fully oxidized Cr samples indicate that there is no unoxidized Cr in the barrier region.

For the fully oxidized Cr junctions of Fig. 3, the background is small for the control junction, but extremely small quantities of Cr_2O_3 in the tunneling region cause large changes in the slope of the linear conductance background. A plot of this slope, measured with the Al electrode 25-mV positive relative to the Pb electrode, versus mass thickness of Cr deposited, for one such set of junctions is shown in Fig. 4. We have made several such sets of junctions. Our control of Cr thickness is poor on the scale of a few Å, so that the mass thickness that gave the largest slope varied by a few Å from run to run, and the peak slope also varied from run to run, but the qualitative features shown here were reproduced. The slope starts at $\simeq 0.03\%/\text{mV}$ for the control sample, rises rapidly with Cr thickness to a maximum of $\simeq 15\%/\text{mV}$ at about 10 Å, and then falls off with increasing thickness to a limiting value of $\simeq 2\%/\text{mV}$. This limiting value at large Cr thicknesses is in agreement with the value obtained for junctions made by oxidizing thin films composed only of chromium.

It could be argued that the linear conduction background in the Al-Al_2O_3-Cr_2O_3-Pb junctions is due to diffusion of Cr into the Al. There are several indications that significant quantities of Cr have not diffused into the Al film under our junction fabrication conditions. First, the saturation concentration of Cr in Al is only 0.3 at. %.[29] Second, very small concentrations of Cr in Al depress its superconducting critical temperature significantly.[30] The resistive transitions of the Al films making up one set of junctions were measured in the same cooldowns as for the current-voltage measurements: no significant difference between the resistance transitions of these films with and without Cr evaporated on them was observed. The third piece of evidence for minimal Cr incorporation in the Al films is displayed in Fig. 5. Figure 5(a) shows conductance-voltage characteristics for a set of junctions with very thin deposits of Cr on them. The control junction with no Cr evaporated on it shows a high-quality superconductor-insulator-superconductor characteristic with conductance peaks at the sum of the gap voltages for Al and Pb. However, superimposed on the expected conductance characteristics are small periodic peaks in conductance. Figure 5(b) shows a Fourier transform of the conductance-voltage characteristics in Fig. 5(a), excluding the gap region from -2 to $+2$ mV. The first peak in these transforms corresponds to voltage spacings of ~ 0.15 meV—the Al gap voltage. We interpret these peaks as due to charging effects between individual grains in the Al films. The important feature of this data for our purposes is that the spacing of these peaks does not change when Cr is included in the barrier region—further indication that there is not significant diffusion of the Cr into the Al films.

However, as can be seen in Fig. 5(a), extremely small

quantities of Cr in the barrier region reduce the size of the gap in conductance due to tunneling between the Al and Pb by about the Al gap value. We interpret this as an indication that magnetic interactions sufficiently strong to suppress the Al gap signature are occurring in tunneling through the Cr_2O_3.[31]

It is striking that the slope of the linear conductance background in these junctions peaks so sharply at a Cr mass thickness of about 10 Å. Unusual magnetic effects have been predicted[32] and observed[33,34] for ultrathin layers of magnetic materials on metallic substrates. Independent of the origin of this peak in slope with Cr_2O_3 thickness, these experiments show that there is a strong linear conductance background in the Al-Al_2O_3-Cr_2O_3-Pb junctions under conditions where it is unlikely that there is significant modification of the composition of the counterelectrodes. This is a strong argument that inelastic tunneling with excitations of modes in the barrier region is responsible for this effect, at least in these samples.

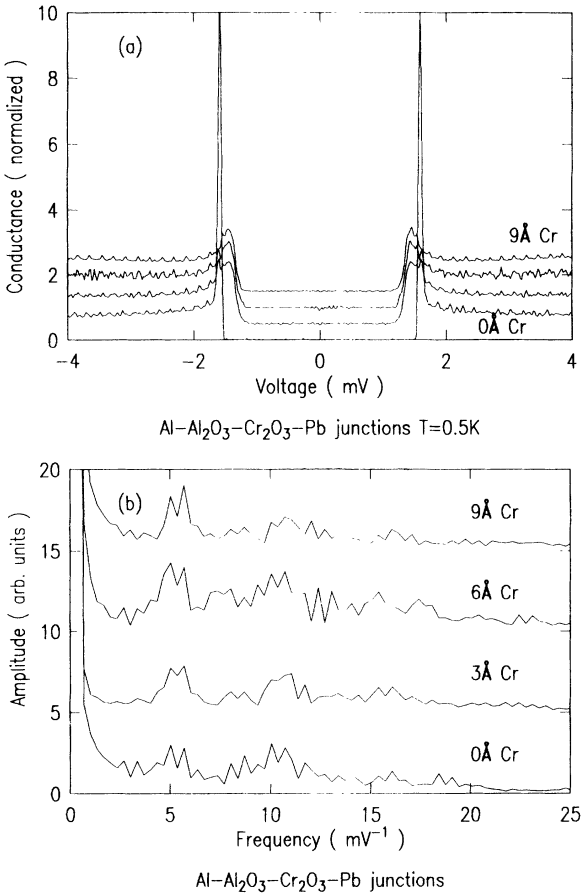

FIG. 5. Low-voltage dynamic conductance curves for a set of Al-Al_2O_3-Cr_2O_3-Pb junctions with mass thicknesses of 0, 3, 6, and 9 Å of Cr on them, respectively. Each successive curve has been offset by 1 unit for clarity. The inclusion of Cr_2O_3 in the barrier region suppresses the Al gap signature in tunneling between the Al and Pb, but has little influence on the small periodic structures which we associate with transport between grains in the Al films themselves. (b) Fourier transforms of the data of (a), excluding the regions between ±2 mV. The peak at about 6 mV^{-1} and its harmonics correspond to the small periodic structures visible in (a). They have a spacing of approximately 0.15 mV, the Al gap value. The position and amplitude of these peaks are relatively unchanged by inclusion of Cr_2O_3 in the barrier region, which we interpret to mean that the bulk superconductivity of the Al films is unaffected.

One concern regarding our interpretation of the linear conductance background is that inelastic tunneling might be expected to broaden in energy or reduce in intensity such elastic features as the peak in conductance at the superconducting energy gap voltage, or the fine structure due to strong-coupling electron-phonon interactions in Pb.[22] This concern has an historical basis, since the study of the linear conduction background in Cr-Cr_2O_3-Pb junctions by Shen and Rowell reported significantly reduced Pb phonon-feature amplitudes in these junctions compared with Pb-*I*-Pb junctions.[9] In contrast, Rochlin and Hansma reported no significant reduction in the size of these features in their Cr-Cr_2O_3-Pb junctions.[10] We have made a quantitative study of this question by comparing the conductance-voltage characteristics of Al-Al_2O_3-Pb junctions with and without Cr_2O_3 in the barrier region. Figure 6(a) shows the conductance-voltage characteristic for a function with a Cr mass thickness of 8 Å. This sample was chosen for detailed analysis because it shows one of the largest conductance backgrounds we have studied, and should therefore provide a stringent test of our modeling.

It is difficult to make a quantitative comparison of the gap structures of junctions with and without Cr because of the shifting of the tunneling conductance peak by the Al gap voltage with the addition of Cr. Nevertheless, it is clear from Fig. 5(a) that even the junctions with large linear backgrounds have high-quality characteristics in the gap region. As we will show below, this is as expected from the inelastic-tunneling model.

In the $T=0$ limit, and neglecting the momentum dependence of the tunneling matrix elements, the inelastic contribution to the total tunneling conductance is given by

$$I_i(V)=(\alpha G_0/e) \times \int_0^{eV} F(\omega)d(\hbar\omega) \times \int_0^{eV-\hbar\omega} N_1(E)N_2(E+eV-\hbar\omega)dE \ , \quad (2)$$

where α is a constant, G_0 is the zero-bias conductance of the junction in the normal state, and N_1 and N_2 are the effective tunneling densities of states of the first and second metal electrodes, respectively. Using Eqs. (1) and (2), and assuming $N_2(E)=1$ (and thereby ignoring small Coulomb effects at very low temperatures which we will discuss later), the total conductance can be written as

$$\frac{dI(V)}{dV}=G_0N_1(eV)+\frac{1}{e}\int_0^{eV} d(\hbar\omega)N_1(eV-\hbar\omega) \times \frac{d^2I_n}{dV^2}(V=\hbar\omega/e) \ , \quad (3)$$

where d^2I_n/dV^2 is the second derivative of the junction current-voltage characteristic in the normal state. The dotted curve in Fig. 6(a) is the conductance of the junc-

tion with a field of 1 T, sufficient to suppress the superconductivity of the Pb. We can infer $F(\omega)$, the spectral density of inelastic excitations from this data through Eq. (1). The superconducting density of states of the Pb is inferred in the conventional way from a control junction with no Cr_2O_3 in the barrier region:

$$N_1(E)=G_0^{-1}\frac{dI(V=E/e)}{dV} . \quad (4)$$

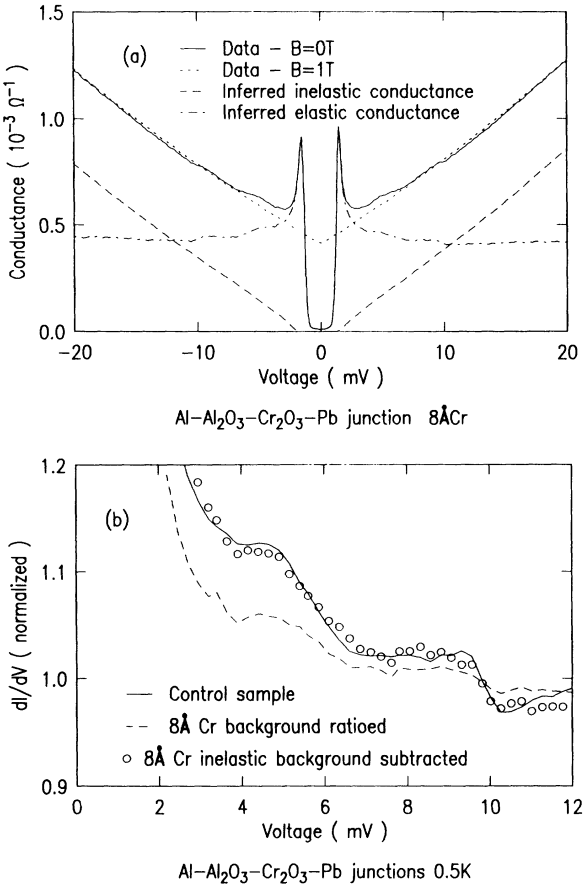

FIG. 6. (a) Dynamic conductance of a thin-film Al-Al_2O_3-Cr_2O_3-Pb junction with 8 Å of Cr evaporated on Al before oxidation. The solid line is the data taken at 0 field and a temperature of 0.5 K. The dotted curve is with a field of 1 T applied normal to the plane of the junction to suppress the Pb superconductivity. The dashed curve is the inelastic component of the total conductance, inferred as described in the text. The dot-dashed curve is the elastic component of the conductance, obtained by subtracting the inelastic background from the total conductance. (b) Comparison of the results of two different normalization schemes on the conductance-voltage characteristics of Al-Al_2O_3-Pb junctions in the voltage region of the strong-coupling Pb phonons. The solid line is from a control sample with no Cr_2O_3 in the barrier region, which has a very small linear conductance background. The open circles are the data from the junction of (a), with the large linear inelastic-tunneling background subtracted out. The agreement between the control sample and the sample with the large background subtracted out is excellent. The dashed curve shows that the conventional normalization, taking the ratio of the conductance in the superconducting to the normal states, is a much worse approximation.

The dashed line in Fig. 6(a) is the inelastic contribution to the total conductance in this junction obtained by numerically integrating the second term in Eq. (3) using (1) $F(\hbar\omega)$ obtained from the 8 Å Cr (sample) junction in the normal state, (2) $N_1(E)$ from the 0 Å Cr (control) junction, and (3) taking $N_2(E)=1$. Note that the scaling factor of the inelastic contribution is uniquely determined in this procedure, given the ratio of zero-bias conductances of the sample and control junctions in the normal state. The dot-dashed curve in Fig. 6(a) shows $I_e(V)$, the elastic component of the conductance for this junction, obtained by subtracting the inelastic component from the total conductance. Figure 6(b) compares this inferred elastic conductance for our sample junction (solid line) with the measured conductance of the control sample (open circles) in the region of the Pb phonon features. The agreement is remarkably good, indicating no broadening or reduction in intensity of these features by the inelastic-tunneling background. It is clear from Fig. 6(a) why the inelastic-tunneling conductance neither contributes to modification of the gap features, nor to smearing of the phonon density-of-states features. Since the inelastic-tunneling contribution is an integral over a broad, featureless continuum, the background to be subtracted has no structure to interfere with the phonon density-of-states features. In addition, since the integral is zero at the gap-edge voltage, no modification of the gap structure results. The dashed line in Fig. 6(b) shows comparable results if the "standard" procedure, dividing the sample junction conductance in the superconducting state by that in the normal state, is used. This is the procedure that Shen and Rowell used in analyzing their data[9] and gives reduced apparent sizes for the phonon features for the junction with Cr in the barrier region as opposed to that without. This procedure is appropriate if the conductance background is due to a reduction of the effective tunneling barrier height by applied bias. Clearly the analysis using the inelastic-tunneling hypothesis, and subtracting out the background conductance, gives better agreement between the sample and control junctions than the "standard" procedure of normalizing by the normal-state conductance.

Further evidence for strong inelastic scattering in the barrier region of the Cr-Cr_2O_3-Pb junctions comes from an analysis of the magnetic field dependence of the linear conduction background. Figure 7(a) shows the low voltage conductance of a Cr-Cr_2O_3-Pb junction at $T=10$ mK in fields of 1 and 14.8 T, with the field oriented normal to the plane of the junction. Very similar results were obtained with the field parallel to the plane of the junction. A field of 1 T was applied for the "baseline" characteristic to suppress features due to superconductivity of the Pb. The $G(V)$ characteristic at 1 T had a discontinuity in the slope of the conductance limited in sharpness only by thermal $5.4kT$ smearing down on temperatures of $\simeq 0.5$ K. Below this temperature an additional small decrease in conductance about 0.2 mV wide appeared. This feature, which is just visible in the data of Fig. 7(a), had a temperature dependence much different from that of the linear conductance background, and was unaffected by the application of fields up to 15 T. Similar features have

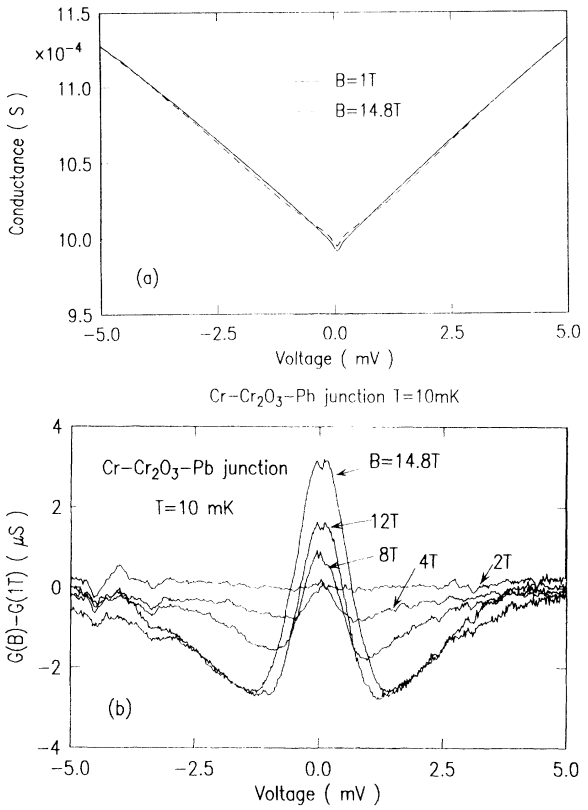

FIG. 7. (a) Dependence of the conductance on magnetic field of a thin-film Cr-Cr_2O_3-Pb junction at a temperature of 10 mK. (b) Difference curves of the conductance of the junction of (a) at various fields minus the conductance at a field of 1 T.

been attributed to Coulomb effects.[35] Subtraction of the $G(V)$ characteristics with different applied fields almost completely eliminated this zero-bias feature.

Figure 7(a) shows that the application of a large field to the Cr-Cr_2O_3-Pb junction caused a slight increase in conductance at zero bias, accompanied by a slight decrease in conductance at intermediate biases. The conductance at high bias was unaffected by an applied magnetic field. Previous attempts to measure the magnetic field dependence of the conductance in these types of junctions[9,10] were not made at sufficiently high fields and low temperatures to observe the effects reported here. The influence of magnetic field on the conductance is made more clear by subtracting the conductance-voltage characteristics at various fields from that at 1 T. The results are shown in Fig. 7(b). The difference curves show peaks that become progressively stronger and wider with larger applied field, with voltage widths $\sim 4\mu_B B$. The presence of structure in the conductance-voltage characteristics with this energy scale is suggestive of Zeeman splitting. Both this magnetic field dependence and the suppression of the Al gap signature by addition of very small quantities of Cr to the interface lead us to explore the possibility that the source of the broadband inelastic scattering is antiferromagnetic magnons.

In the limit $T=0$ in two dimensions, the antiferromagnetic magnon spectral density can be written as

$$F(\omega)=\sum_q \frac{2ZJ}{\omega(q)}\delta(\omega-\omega(q)) , \tag{5}$$

where Z is the number of nearest neighbors, J is the antiferromagnetic coupling strength, and the sum is over in-plane wave vectors q and the two branches of the dispersion curves. The use of the two-dimensional form for the spectral density is justified at low energies for our thin Cr_2O_3 films because the higher branches associated with nonzero wave vectors in the direction normal to the plane of the junction are close to the zone edge energy — $\simeq 40$ meV in Cr_2O_3.[37] We will discuss the linear conduction background at high-voltage biases below. The expected dispersion relation $\omega(q)$ for antiferromagnetic magnons is illustrated in Fig. 8.[38] For this figure we have taken an exchange energy of 40 meV,[37] an anisotropy gap of 0.6 meV,[37] and a g factor of 1.97,[36] suitable for Cr_2O_3. In zero field the dispersion curve (solid line in Fig. 8) is linear above the anisotropy gap energy until it approaches the exchange energy value at the zone edge. At finite fields (dashed curves in Fig. 8), the dispersion curves split by $\pm g\mu_B H$ until the lower branch crosses zero energy at the "spin-flop" field. In Cr_2O_3 this field is about 6 T.[39] Above the spin-flop field, dispersion curves like the dashed lines in the insert of Fig. 8 result. Above the spin-flop field the dispersion curves are split by $g\mu_B H$ at $q=0$.

The existence of a gap in the spin-wave excitation spectrum at low energies might be expected to cause a flattening of the linear conduction background at low voltages. We see no indications of such a flattening in our Cr-Cr_2O_3-Pb junctions down to voltages of 1 mV. However, simple modeling indicates that a spin-wave coherence length of about 100 lattice constants would be required to observe this effect. It is unlikely that our amorphous oxides support coherent spin waves over such large distances.

The magnetic field dependences of the linear conduction background displayed in Fig. 7 show a slight increase in conductance near zero bias when a field is ap-

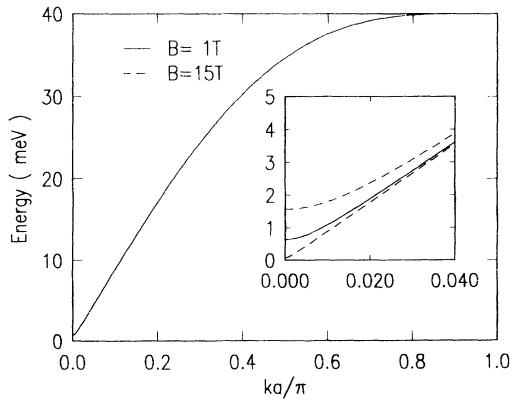

FIG. 8. Representative calculated dispersion curves for the spin-waves of an antiferromagnet with an exchange energy of 40 meV, an anisotropy energy of 0.6 meV, and a g factor of 1.96. The dashed lines in the inset show the splitting of the low-energy part of the two branches of the dispersion curve upon application of a 15-T field.

plied. The fact that this is just opposite to the magnetic field behavior noted for junctions with strong zero-bias anomalies[9] make us believe that the effect described here involves a different physical mechanism. Standard treatments of inelastic tunneling[40,24,41] add the inelastic conductance to a constant elastic conductance. In our case this would imply no change in conductance at zero bias with magnetic field, since the conductance at zero bias is completely elastic. However, Persson[42] has shown that inelastic tunneling can take conductance away from the elastic channel. He considers a harmonic oscillator in the barrier region interacting with a tunneling electron. The probability $P_n(\xi)$ of the oscillator finishing in the nth excited state as a function of the strength of the interaction ξ is given by

$$P_n(\xi)=\xi^n\frac{e^{-\xi}}{n!}\ . \tag{6}$$

In the limit of small interaction strength ξ, the elastic component is proportional to $P_0(\xi)=1-\xi$, and the inelastic component is proportional to $P_1(\xi)=\xi$. There is then a "sum rule" where, in our case, the conductance lost in inelastic scattering due to the opening of the gap by application of a magnetic field is compensated by a gain in conductance in the elastic channel. This has the effect that our predicted conductance-voltage curves at different fields overlap at high voltages, in agreement with experiment.

Figure 9 shows the prediction of simple spin-wave theory for the field dependence of the linear conduction background, which we obtain by integrating the spectral distribution function $F(\omega)$ of Eq. (5) following Eq. (1), and using the "sum rule" discussed above. The dispersion curves used were calculated following Jones *et al.*,[38] within an exchange energy of 40 meV, and an anisotropy energy of 0. Using finite anisotropy gap energies in these calculations puts additional structure into the predicted difference curves, but does not change them qualitatively. Note first that the zero-field conductance curves are predicted to be linear at low voltage, in agreement with experiment. This results from the linearity of the dispersion curves at low energies, combined with the cancellation of the factor of q obtained by integrating over the two-dimensional density-of-states factor, by the $\omega^{-1}\sim q^{-1}$ factor in Eq. (5). The magnetic field dependence of the linear conduction background predicted by simple spin-wave theory agrees qualitatively with experiment. The voltage widths of the changes in conductance are in good agreement with experiment, but the absolute magnitude of the peak to dip change in conductance with applied field is about a factor of 3.5 smaller than predicted by our model. Modeling shows that reduced spin-wave coherence lengths tend to reduce the predicted amplitudes, in better agreement with experiment. The characteristic undershoots seen in experiment, which might be expected to be present in the modeling from the form of the magnetic field induced gap seen in Fig. 8, tend to be suppressed by the ω^{-1} factor in Eq. (5). Nevertheless, the qualitative agreement between theory and experiment lends support to the notion that spin excitations are involved in the linear conduction background in these junctions.

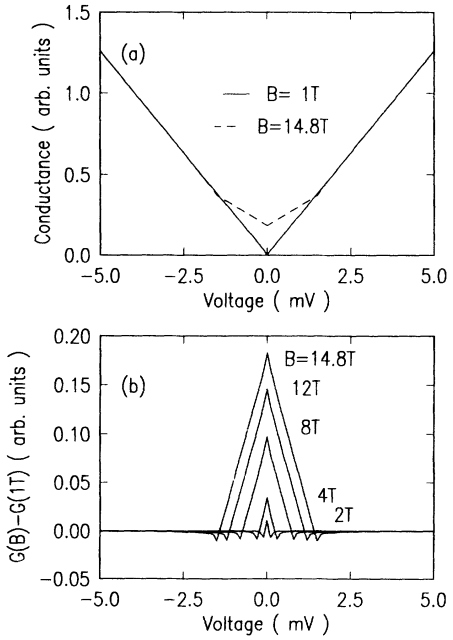

FIG. 9. Predictions of our model for the low-voltage conductance background due to inelastic electron tunneling with excitation of spin waves, at fields of 1 and 14.8 T and temperatures of 0 K. The bottom half of the figure shows the difference curves for the same fields as displayed in the experimental curves in Fig. 7(b).

One difficulty in ascribing the broadband inelastic tunneling observed in our Cr-Cr_2O_3-Pb junctions to excitations of spin waves is that the linear conduction background extends out to at least 200 mV, higher than the maximum spin-wave energy in Cr_2O_3. This is a general problem: the linear conduction background extends to energies[1] beyond those of the elementary excitations, e.g., phonons, magnons, charge-density waves, that might be excited in the inelastic scattering. Similar difficulties are experienced in understanding the broad scattering background often observed in Raman scattering from the high-T_c superconductors.[8] This may imply that multiple emission processes are involved in both cases. Kirtley and Soven,[43] in multiple-scattering calculations of inelastic tunneling from CO molecules included in the barrier region of planar tunnel junctions, showed that the inelastic-tunneling cross sections can become extremely large when the tunneling electron energy matches a bound-state energy of the included molecules. They also showed that, at least in the absence of strong coupling between the included molecules and one of the metal electrodes,[42] emission of multiple excitations becomes likely when the resonance condition is met. These resonances are not necessarily narrow: for CO the lowest-lying resonance in the inelastic-tunneling cross section is calculated to be of order 1 eV wide.[43] Resonance inelastic tunneling can therefore explain two puzzling features in the linear conduction background; the extremely large size of the effect and the wide voltage range over which it occurs.

The calculation of the linear conduction background

due to multiple inelastic tunneling with the emission of spin waves is a formidable challenge. For this paper we take the simplest possible approach to see what qualitative features emerge. To this end we make several simplifying assumptions. We assume that the magnon scattering occurs only in a plane a distance 5 Å from one of the sides of a square potential barrier 2 eV high and 20 Å wide. The initial and final wave functions are taken to be of the standard decaying plane wave WKB form[41] on opposite sides of the barrier. We take the spatial dependence of the interaction Hamiltonian to be given by δ functions localized at the nuclear spin sites. This results in inelastic-tunneling matrix elements which are proportional to the product of the amplitudes of the initial and final wave functions, with appropriate energy and momentum-conserving δ functions.[24] We take the probability $P_n(\xi)$ for excitation of n magnons to be given by Eq. (6), and use Monte Carlo techniques to sum the matrix elements over all possible initial electron, final electron, and magnon momenta, preserving energy and momenta in the scattering processes. Qualitatively similar results are obtained if momentum is not assumed to be conserved in the scattering process (incoherent scattering[24]). Typical results, summed out to fifth order in the magnon emission, are presented in Fig. 10. The top part of the figure shows $P(E)$, the relative probability that a tunneling electron with zero initial energy relative to the left-hand Fermi energy will finish with final energy $-E$ on the right-hand side of the tunneling barrier, for various values of the interaction strength ξ. Each curve sums the results of 120 000 trials. Zero energy loss corresponds to elastic tunneling. These probabilities are normalized by the probability for tunneling with no loss. There are several features of interest in these scattering distributions. At low interaction strengths the energy losses are dominated by first-order scattering, and there is a sharp peak at the magnon zone boundary energy of 40 meV. As the interaction strength ξ increases, higher-order processes gain weight, and the distribution function starts to look relatively flat. The peaks at multiples of 40 meV become less distinct for higher-order scattering.

In the limit where the barrier height is much higher than both the energy losses and the voltage bias, $P(E)$ is proportional to the spectral distribution function $F(\hbar\omega)$. At $T=0$, Eq. (1) holds and the tunneling conductance is proportional to the integral of $P(E)$. This is shown in the bottom half of Fig. 10. The sharp steps in conductance in these curves arise from the sharp peaks in our assumed spin-wave density of states at the zone edges. Anisotropy,[37] spatial inhomogeneities, finite-lifetime effects, and magnon-magnon interactions[44] are expected to broaden these features. Aside from these steps, the predicted conductance appears relatively linear for large interaction strengths. These calculations therefore make it plausible that the linear conduction background at high voltages comes from multiple-scattering processes.

An additional feature of the Monte Carlo simulations in Fig. 10 is that they are asymmetric. The sense of the asymmetry is such that the conductance is larger for electrons tunneling in a direction where the scattering centers are closest to the final metal electrode. An interesting property of this asymmetry is that the conductance-voltage curves for opposite biases overlap well when a constant scaling factor is used: the asymmetry is not strongly voltage dependent. This is consistent with what is observed experimentally in the linear conduction background (see, for example, Fig. 1). This is in contrast to the asymmetry observed in discrete mode IETS, where the ratio of peak heights for the two opposite bias directions depends nearly linearly on the voltage, and approaches unity at zero voltage.[41] In discrete mode IETS, the source of the asymmetry is the difference in the barrier penetration probabilities before and after scattering due to the energy loss upon scattering. If the scattering centers are closer to one barrier than the other, there will be asymmetry in the size of the IETS peaks.

The source of the asymmetry in our Monte Carlo simulations of broadband inelastic tunneling is similar to that for discrete mode IETS, but with a subtle difference. The magnon emission processes included in our simulation are dominated by large momentum transfer scattering. Therefore, electrons are less likely to tunnel if they scatter before penetrating most of the barrier than if they scatter after penetrating most of the barrier. This difference in the barrier penetration probabilities is rela-

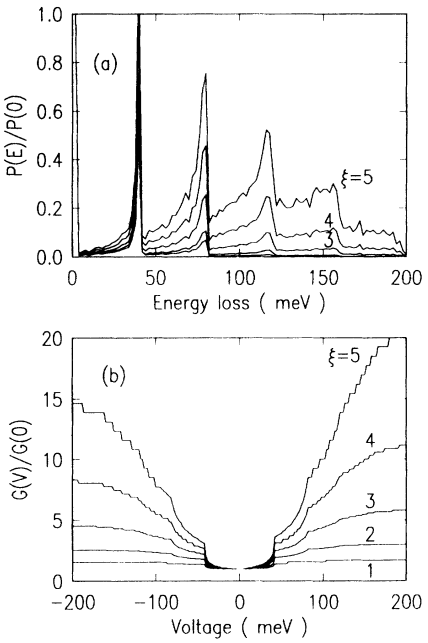

FIG. 10. The results of the Monte Carlo calculations for inelastic tunneling with multiple excitation of spin waves. The upper figure shows the distribution of energy losses of the tunneling electrons, for interaction strengths $\xi=1$, 2, 3, 4, and 5. Larger interaction strengths result in stronger scattering at higher energy losses. The lower part of the curve shows the resulting conductance curves, normalized to the elastic tunneling. Aside from sharp steps in conductance resulting from the singularities in our assumed spin-wave density of states, the conductances are fairly linear at high-voltage biases for large interaction strengths. The predicted curves are also asymmetric with respect to the tunneling direction. This asymmetry has some of the unusual properties of the asymmetry observed experimentally.

tively independent of the energy loss, and therefore the asymmetry ratio for opposite voltage biases will be relatively voltage independent. For discrete mode IETS, the scattering is dominated by long-range dipole interactions which transfer relatively little transverse momentum to the tunneling electron, and so the major source of differences in the barrier penetration probabilities is due to the energy loss, and the asymmetry ratio is voltage dependent.

Unfortunately, the sign of the asymmetry predicted by our Monte Carlo calculations is just opposite to that which is most plausible from our limited experimental evidence. Consider the data from the Al-Al_2O_3-Cr_2O_3-Pb junctions presented in Fig. 3. Here the sign of the asymmetry is such that the conductance is higher when electrons tunnel into the Al electrode from the Pb. From the order in which the metals were evaporated it appears most plausible that the scattering centers in the Cr_2O_3 are closest to the Pb electrode, so the experimentally preferred tunneling direction has the electrons penetrating the majority of the tunneling barrier after scattering. This implies that there is something wrong with our reasoning—either the positioning of the scattering centers is not as we think, or our simple calculation does not have the scattering quite right. Note, however, that in the more rigorous multiple-scattering calculations of Kirtley and Soven for inelastic vibrational mode tunneling through CO,[43] either sign of the asymmetry is possible, depending on the energy of the tunneling electron relative to the resonance energy (see Fig. 2 of Kirtley and Soven[43]). Therefore, it should not be too disappointing that our simple modeling does not get the sign of the asymmetry correct in the present case.

In conclusion, we have presented evidence in support of the view that the linear conduction background is due to inelastic electron tunneling from a broad distribution of loss modes. The evidence is particularly compelling when junctions with Cr_2O_3 in the barrier region are studied in detail: the temperature dependence, and an analysis of strong-coupling Pb phonon features are consistent with this interpretation: the dependence of the strength of the effect on barrier composition argues strongly in favor of this interpretation. The suppression of the Al gap feature in tunneling, and the magnetic field dependence of the linear background, indicate that spin interactions are involved in the tunneling process in junctions with Cr_2O_3 in the barrier region. Monte Carlo simulations make it plausible that the background conductance at large biases involves multiple emission processes, and provides an explanation for the unusual asymmetry in the linear conduction background with opposite voltage biases.

We have concentrated in this paper on junctions with Cr_2O_3 in the tunneling barrier, but tunneling into the high-T_c superconductor shows absolute magnitudes for the size of the conductance background in the same range as those displayed here, and the same smearing of the discontinuity in conductance at zero bias with temperature. It appears likely that strong broadband inelastic electron tunneling is active in these cases as well.

We would like to thank R. T. Collins, L. Rotter, P. K. Hansma, R. C. Dynes, M. V. Klein, and M. Buettiker for helpful discussions.

[1]Mark Lee, M. Naito, A. Kapitulnik, and M. R. Beasley, Solid State Commun. **70**, 449 (1989).
[2]M. Gurvitch *et al.*, Phys. Rev. Lett. **63**, 1008 (1989).
[3]P. W. Anderson and Z. Zou, Phys. Rev. Lett. **60**, 132 (1988).
[4]C. M. Varma, P. B. Littlewood, S. Schmitt-Rink, E. Abrahams, and A. E. Ruckenstein, Phys. Rev. Lett. **63**, 1996 (1989).
[5]J. C. Phillips, Phys. Rev. B **41**, 8968 (1990).
[6]J. R. Kirtley and D. J. Scalapino, Phys. Rev. Lett. **65**, 798 (1990).
[7]R. T. Collins, Z. Schlesinger, F. Holtzberg, P. Chaudhari, and C. Field, Phys. Rev. B **39**, 6571 (1989).
[8]S. L. Cooper, M. V. Klein, B. G. Pazol, J. P. Rice, and D. M. Ginzberg, Phys. Rev. B **37**, 5920 (1988); S. L. Cooper *et al.*, *ibid.* **38**, 11 934 (1988).
[9]L. Y. L. Shen and J. M. Rowell, Phys. Rev. **165**, 566 (1968).
[10]G. I. Rochlin and P. K. Hansma, Phys. Rev. B **2**, 1460 (1970).
[11]F. Mezei, Phys. Lett. **25A**, 534 (1967).
[12]A. F. G. Wyatt and D. J. Lythall, Phys. Lett. **25A**, 541 (1967).
[13]See, e.g., M. F. Muldoon, R. A. Dragoset, and R. V. Coleman, Phys. Rev. B **20**, 416 (1979).
[14]J. E. Christopher, R. V. Coleman, Acar Isin, and R. C. Morris, Phys. Rev. **172**, 485 (1968).
[15]W. J. McMillan and Jack Mochel, Phys. Rev. Lett. **46**, 556 (1981).
[16]R. T. Collins, J. Lambe, and T. C. McGill, Appl. Phys. Lett. **44**, 533 (1984).
[17]J. R. Kirtley, Int. J. Mod. Phys. B **4**, 201 (1990).
[18]J. R. Kirtley *et al.* Phys. Rev. B **35**, 7216 (1987).
[19]S. Pan, K. W. Ng, A. L. de Lozanne, J. M. Tarascon, and L. H. Greene, Phys. Rev. B **35**, 7220 (1987).
[20]R. Medina, J. Aponte, and M. Octavio, Physica B **165**, 1595.
[21]H. R. Zeller and I. Giaever, Phys. Rev. **181**, 789 (1969).
[22]J. M. Valles, Jr., R. C. Dynes, A. M. Cucolo, M. Gurvitch, L. F. Schneemeyer, J. P. Garro, and J. V. Waszczak, Phys. Rev. B **44**, 11 986 (1991).
[23]R. C. Jaklevic and J. Lambe, Phys. Rev. Lett. **17**, 1139 (1966).
[24]C. B. Duke, S. D. Silverstein, and A. J. Bennett, Phys. Rev. Lett. **19**, 315 (1967).
[25]P. Dutta, P. Dimon, and P. M. Horn, Phys. Rev. Lett. **43**, 646 (1979).
[26]A good review of IETS appears in *Tunneling Spectroscopy: Capabilities, Applications, and New Techniques,* edited by P. K. Hansma (Plenum, New York, 1982).
[27]J. D. Langan and P. K. Hansma, Surf. Sci. **52**, 211 (1975).
[28]S. T. Ruggiero and J. B. Barner, Phys. Rev. B **36**, 8870 (1987).
[29]R. P. Agarwala, S. P. Murarka, and M. S. Anand, Acta Metall. **12**, 871 (1964).
[30]O. F. de Lima, Y. Lepetre, and M. B. Brodsky, in *Interfaces, Superlattices, and Thin Films,* edited by J. K. Dow and I. K. Schuller, MRS Symposia Proceedings No. 77 (Materials Research Society, New York, 1987).
[31]Peter Fulde and R. A. Ferrell, Phys. Rev. **135**, A550 (1964).
[32]C. L. Fu, A. J. Freeman, and T. Oguchi, Phys. Rev. Lett. **54**, 2700 (1985).

[33]J. S. Moodera and R. Meservey, Phys. Rev. B **40**, 8541 (1989).
[34]M. C. Hanf, C. Pirri, J. C. Peruchetti, D. Bolmont, and G. Gewinner, Phys. Rev. B **39**, 1546 (1989).
[35]Waldemar Maj, Solid State Commun. **74**, 395 (1990).
[36]Simon Foner, Phys. Rev. **130**, 183 (1963).
[37]E. J. Samuelson, M. T. Hutchings, and G. Shirane, Physica **48**, 13 (1970).
[38]D. H. Jones, Q. A. Pankhurst, and C. E. Johnson, J. Phys. C **20**, 5149 (1987).
[39]Y. Shapira, Phys. Rev. **187**, 734 (1969).
[40]D. J. Scalapino and S. M. Marcus, Phys. Rev. Lett. **18**, 459 (1967).
[41]J. Kirtley, D. J. Scalapino, and P. K. Hansma, Phys. Rev. B **14**, 3177 (1976).
[42]B. N. J. Persson, Phys. Scr. **38**, 282 (1988).
[43]John Kirtley and Paul Soven, Phys. Rev. B **19**, 1812 (1979).
[44]R. J. Elliott and M. F. Thorpe, J. Phys. C **2**, 1630 (1969).